BMC Genomics

RESEARCH Open Access

# Gene expression and immune cell heterogeneity in inbred Amur tiger

Jinping Bi[1,2†], Xiaoyun Hu[1†], Dejun Mu[3†], Chang Liu[3†], Kai Wang[4], Yong Yao[5], Dan Jin[3], Junguang Lu[3], Yifei Zhang[1,2], Yao Ning[1,2*] and Jiang Feng[1,6*]

## Abstract

Inbreeding leads to a reduction in genetic diversity and an elevated likelihood of expressing recessive defective genes, which adversely affect the development of the immune system and render individuals and populations more susceptible to carcinogenic factors, consequently heightening the risk of cancer. Through investigating the function and extent of immune cell interaction in peripheral blood mononuclear cells (PBMCs) of inbred individual, a comprehensive understanding can be gained regarding the impact of inbreeding on various aspects of the immune system, including diversity, self-tolerance, immune responsiveness, susceptibility to diseases, and other related areas. Currently, the wild Amur tiger population in China exhibits a moderate degree of inbreeding, with a probability exceeding 90% that it will be deemed extinct within the forthcoming century. However, the impact of inbreeding on the immune system remains ambiguous, presenting numerous challenges for the development and implementation of conservation strategies. Here, for the first time, a detailed single-cell sequencing atlas of peripheral blood samples obtained from Amur tigers is presented, delineating eight distinct cell types. Our study demonstrates that the inbred tiger exhibits a relatively lower proportion of lymphocytes and cDC2 cells, along with reduced intercellular interactions. We also observed elevated activity in several signaling pathways (e.g., TGFb, APRIL, BAG, GRN, VISFATIN) that have been linked to inflammation and cancer in other species. The WGCNA analysis analysis further suggested a candidate regulatory network in inbred tiger, with the cancer-associated gene *YTHDC2* emerging as a hub gene. Together, our exploratory study offers preliminary insights into the immune heterogeneity in inbred Amur tigers and can potentially guide future studies aimed at enabling timely health interventions for this endangered species.

**Keywords** Inbred, Immunity, Amur tiger, PBMCs, scRNA-seq

†Jinping Bi, Xiaoyun Hu, Dejun Mu and Chang Liu contributed equally to this work.

*Correspondence:
Yao Ning
yaoning1001@126.com
Jiang Feng
fengj@nenu.edu.cn

[1]College of Life Science, Jilin Agricultural University, Changchun, Jilin, China
[2]Jilin Provincial International Cooperation Key Laboratory for Biological Control of Agricultural Pests, Changchun, Jilin, China
[3]Changchun Zoological and Botanical Park, Changchun, Jilin, China
[4]Liaoning Qianshan Tourism Group Co, Anshan, Liaoning, China
[5]Chongqing Zoo, Chongqing, China
[6]Jilin Provincial Key Laboratory of Animal Resource Conservation and Utilization, Northeast Normal University, Changchun, Jilin, China

## Introduction

Global habitat loss and fragmentation have led to the isolation of many wildlife populations, restricting genetic exchange and increasing the likelihood of inbreeding [1]. The core genetic hazard of inbreeding is that it significantly increases the probability of homozygous recessive deleterious alleles [2, 3]. When these originally masked harmful genes are expressed, a series of "inbreeding depression" phenomena will be triggered, which will seriously damage the survival and reproductive ability of individuals [4]. Among them, the significant decline in immune system function is considered to be one of the most prominent and destructive consequences of inbreeding depression. A large number of studies have confirmed that inbred individuals often show a decline in key immune indicators, such as decreased antibody response, inflammatory response disorders, or a decrease in the number of specific immune cells [5–7]. These immunodeficiencies directly weaken the individual's ability to resist the invasion of pathogens. For example, the inbreeding of American crows (*Corvus brachyrhynchos*) has been linked to high mortality rates from vector-borne diseases such as West Nile virus and avian malaria [8]. Similarly, Reid et al. found that the 6-day-old chicks of song sparrows (*Melospiza melodia*) showed decreased cell-mediated immune response (CMI) when their mothers had higher inbreeding coefficients, while adult sparrows showed decreased CMI related to their inbreeding levels [9]. Therefore, inbreeding not only brings about the loss of genetic diversity but also directly leads to a sharp rise in the overall disease susceptibility of small and isolated populations. The weakening of immune adaptability is the core link in this vicious cycle.

As the core defense line for organisms to resist pathogen invasion and maintain health, a sound immune system is crucial for the survival of individuals and the continuation of populations [10, 11]. It removes foreign pathogens and forms immune memory to cope with future threats through complex cellular and molecular network recognition [9]. However, inbreeding has caused systemic damage to this key barrier, which is mainly reflected in: the diversity of immune cell banks is reduced, which limits the ability to recognize broad-spectrum pathogens [12]; specific antibody responses to new pathogens become slow and narrow [13]; more seriously, the overall weakening of immune adaptability will damage the function of immune surveillance [14]. Immune surveillance is a key mechanism for the immune system to recognize and clear cancerous cells in vivo. When this function is weakened by inbreeding, the risk of abnormal cells escaping from clearance and developing into tumors is significantly increased. Accordingly, inbreeding not only increases the susceptibility to infectious diseases by reducing the anti-infective ability but also indirectly increases the risk of cancer by weakening the immune surveillance function, posing a dual threat to population health. The weakening of immune adaptability is the internal driving factor for the increase of disease susceptibility in inbreeding populations. In order to further reveal its molecular mechanism, scientists are actively using cutting-edge tools such as single-cell transcriptome technology. This technology can not only accurately identify immune cell subsets and their phenotypic changes through gene expression characteristics, but also analyze intercellular communication networks (such as cytokine-receptor interaction) [15], thus revealing the functional abnormalities and regulatory mechanisms of immune cells in inbred individuals [16], and providing a theoretical basis for targeted intervention.

The Amur tiger (*Panthera tigris altaica*), as the apex predator in mammalian ecosystems, plays a crucial role in maintaining ecological equilibrium and promoting species diversity [17]. Currently, there are currently 70 wild Amur tigers in China, and an analysis utilizing mathematical models based on the current population status predicts a probability exceeding 90% for their extinction within the next century [18, 19]. Simultaneously, this population already demonstrates a moderate degree of inbreeding, consequently engenders an augmented burden of parasitic infections and an elevated abundance of pathogens, as well as profoundly impairing the gut microbiota's biosynthetic, degradative, and utilization functions [20]. However, the impact of inbreeding on the immune systems of wildlife remains inadequately explored, potentially resulting in a diminished capacity for populations to handle sudden ecological challenges, which could lead to elevated mortality rates, further reducing population sizes and ultimately disrupting the ecosystem's equilibrium. Furthermore, due to a thorough study of wild Amur tiger species is challenging due to their limited population size and elusive nature, but captive Amur tigers play a crucial role in conserving their wild counterparts and offer valuable opportunities for extensive research on individuals exhibiting varying degrees of inbreeding.

Summing up, we assume that inbreeding among Amur tigers may induce immune system dysfunction in their progeny, which results in aberrant inflammatory responses and subsequently elevates the risk of cancer. Hence, to corroborate this hypothesis, we employed single-cell transcriptome sequencing to analyze peripheral blood mononuclear cells from both inbred and non-inbred Amur tiger individuals to characterize cell types and perform comparative assessments. The objective of this research is to (1) construct a comprehensive atlas of peripheral blood monocytes in Amur tiger individuals; (2) elucidate the effects of inbreeding on the distribution of immune cell types, their interactions, and the resultant

transcriptomic alterations; (3) identification of critical genes in inbred Amur tiger. The purpose of this study was to clarify the effect of inbreeding on the immune system of the Amur tigers and to provide a reliable database support for assessing the risk of inbreeding disease in the Amur tigers.

## Materials and methods

### Sample collection and treatment

In this study, we observed two 12-month-old female Amur tigers with identical feeding habits in order to minimize the influence of extraneous variables, and the degree of inbreeding within the individual was assessed based on the family pedigree. Venous blood samples were collected from one non-inbred and one inbred individual at Baoshanqian Wild Animal Park and Changchun Zoological and Botanical Park, with an inbreeding coefficient of 0.25 recorded for the inbred individual. Both individuals had not used antibiotics and were in good health for three months before sample collection.

### Calculation of inbreeding coefficient based on ROH

In order to obtain a more accurate inbreeding level of two individuals, 4 mL of whole blood was taken for whole genome sequencing and the inbreeding coefficient of Amur tigers was evaluated by ROH. FASTP 0.23.1 [21] software was used to perform quality control on the sequencing raw data involved in this experiment to remove readings with connections, excess N content, and low quality. The clean data were compared with the reference genome of the Amur tiger (GCF_018350195.1_P.tigris_Pti1_mat1.1) by BWA 2.2.1 [22] software, and then the BAM file was generated after sorting and deduplication steps. Subsequently, the bcftools 1.21 [23] software was used to detect population SNPs in the samples, and 2,769,364 high-quality SNPs were obtained after filtering and screening. The filtering and screening conditions were as follows: the minimum depth of a single SNP in a single sample was 4 bp, the maximum deletion rate was less than 0.1, and the minimum minor allele frequency was 0.05. Finally, the functional annotation of the detected SNPs was performed by ANNOVAR [24] software.

The homozyg parameters of PLINK 1.9 software were used to determine the ROH of the samples, with the parameters set as follows: -homozyg-density 5; -homozyg-window-het 1; -homozyg-window-snp 10-homozyg-kb 100; -homozyg-snp 5. The number and length of ROH fragments and the distribution of ROHs at the genomic and chromosomal levels were obtained for each sample. At the same time, the obtained ROHs were divided into three groups according to the length of ROH: < 1 Mb, 1–5 Mb, and > 5 Mb. The < 1 Mb ROH fragment was defined as a short ROH fragment, the ROH fragment in the 1–5 Mb length range was defined as a medium ROH fragment, and the ROH fragment > 5 Mb was defined as a long ROH fragment. The estimated genomic inbreeding coefficient ($F_{ROH}$) was calculated based on McQuillan [25]: $F_{ROH} = \frac{L_{ROH}}{L_{AUTO}}$. Where $L_{ROH}$ is the total length of ROH for each individual, and $L_{AUTO}$ is the total length of the autosomal genome covered by the SNP (about 2,398,865 kb).

### scRNA-seq library preparation and sequencing

About 4 mL of whole blood was collected from the same batch of blood of each individual using an EDTA tube. Subsequently, the acquired whole blood samples were diluted at a ratio of 1:1 with a buffer of 1640 medium supplemented with 10% FBS (Fetal Bovine Serum). The diluted blood was cautiously injected into the lymphocyte separation medium and centrifuged for 40 min at a temperature of 20℃. After removing the plasma, transfer the lymphocytes to a washing solution containing RPMI 1640 medium with 10% fetal bovine serum, centrifuge the mixture at 20 °C for 5 min, and then monitor the number of precipitated red blood cells. The cellular morphology was recorded by enumerating and capturing images under a microscope once the supernatant was removed and the cells were resuspended in a buffer containing 1640.

Firstly, the cell suspension was placed into Chromium microfluidic chips with 3' chemistry, and a 10x Chromium Controller (10X Genomics) was employed to barcode the chips. Afterward, the RNA from barcoded cells was reverse-transcribed, and sequencing libraries were constructed using the Chromium Single Cell 3' reagent kit (10X Genomics) according to the manufacturer's instructions. Subsequently, high-throughput sequencing was conducted on the Illumina NovaSeq platform.

### Processing of raw scRNA-seq data

The 10XGenomics Cell Ranger pipeline was utilized with default parameters to demultiplex raw data and align it to the reference genome of the Amur tiger in the NCBI database (GCF_018350195.1_P.tigris_Pti1_mat1.1). Subsequently, each gene's unique molecule identifiers (UMIs) were quantified. Then, the star software of Cell Ranger 7.0.0 [26] was used for alignment. After the reads were aligned to the reference genome, the GTF annotation file was used for correction, and the exon region, intron region, and intergenic region were distinguished. The discrimination rule is: at least 50% of the reads aligned to the exon are recorded as the exon region, and the reads aligned to the non-exon region and intersected with the intron region are recorded as the intron region, and the remaining sequences are non-coding regions. Next, Cell Ranger is used to distinguish each cell's reads by the input

data's barcode, and the number of cells in the sample, the number of reads of cell, and the number of detected genes are counted by filtering and screening. The specific steps are as follows: First, a desired number of cells (N, default 3000) is specified, and then the barcodes are sorted from high to low according to their respective UMI totals. The 99% quantile of the first N UMI values is taken as the maximum estimated UMI total (m), and the barcodes with a UMI number exceeding m/10 are used as the final captured cells. Finally, further filtration was performed using Seurat 3.1.0 [27] to remove multiple cells from the dataset to ensure the reliability and accuracy of the subsequent analysis results; the filtration criterion involved removing genes detected in fewer than three cells, as well as cells with gene expression below 200, and filtering out some of the foreign cells.

#### Cell classification

The data standardization process in Seurat involves applying the "LogNormalize" global normalization method to the filtered cell-gene expression matrix, followed by dimensionality reduction and clustering for cell classification. Meanwhile, to align integrated datasets, the canonical correlation analysis (CCA) method [28] was employed as an alignment strategy. Then, clustering was performed using highly variable genes with pronounced expression discrepancy, and a graph was constructed based on principal components derived from these genes. The default value of 0.6 was used for setting the graph's resolution. It should be noted that immune cell subsets in tigers were annotated through comparison with humans or mice. Considering the high conservation of core mammalian immune genes and the lack of a dedicated tiger marker database, this orthology-based approach offers a reasonable and practical strategy for cell type identification. However, it is also crucial to recognize its inherent limitation stemming from potential species specific variation in gene expression and function.

#### Differentially Expressed Gene (DEG) enrichment analysis

Leveraging Seurat's filtered gene expression matrix, differential expression analysis between groups was performed using the edgeR package [29] to discern cluster-specific marker genes. Subsequently, Gene Ontology (GO) [30] and Kyoto Encyclopedia of Genes and Genomes (KEGG) [31] enrichment analyses were conducted on these marker genes using the R package clusterProfiler 3.14.0 [32] with gene length bias corrected via the BH method [33]; a significance threshold of $p < 0.05$ was applied for determining significant enrichment. Additionally, the accuracy of these subpopulation definitions was confirmed through cell trajectory analysis across the entire sample set.

#### Cell trajectory analysis

Based on the pooled dataset of inbred and non-inbred, we performed pseudotime trajectory analysis using the R package monocle 2.32.0 [34] to validate the accuracy of the cell subpopulation classifications. Through the construction of trajectories that depict temporal changes in cells, we aimed to shed light on the dynamic progression of cell states and thereby confirm the precision of cellular subpopulation classifications.

#### WGCNA analysis

In this study, we performed WGCNA analysis to further elucidate the critical genes influencing immunological heterogeneity in inbred individual [35]. Initially, a co-expression network was established for all genes utilizing the R package WGCNA 1.72.5, concentrating on the top 25% of genes ranked by variance and applying a soft threshold parameter set to 18. Construct an adjacency matrix based on inter-gene correlations and then transform the adjacency matrix into a topological overlap matrix (TOM), and hierarchical clustering was employed to generate modules, with each module consisting of genes clustered with a minimum size of 30 [36]. By investigating the relationship between each module and both inbred and non-inbred phenotypes, we identified module genes most significantly associated with inbreeding. Subsequently, KEGG enrichment analysis was conducted on these genes. Additionally, this study employs Cytoscape to visualize gene connections within modules, initially uses the MCODE plug-in to identify the network with the highest score [37], then employs the cytoHubba plug-in to compute node scores, and finally visualizes the top 30 genes [38].

#### Cell communication analysis

To determine the differences in complex cell-cell interactions among multiple cell populations of separate datasets of inbred and non-inbred individuals, we utilized the R software package scDiffcom 1.0.0 [39]. This package relies on approximately 5,000 selected ligand-receptor interactions and performs analysis based on single-cell transcriptome data [40].

## Results

#### ROH analysis and inbreeding coefficient evaluation of inbred and non-inbred Amur tigers

According to the statistical results, the total number of ROH observed in inbred and non-inbred Amur tigers was 1,629 and 805, respectively, and the corresponding total length of ROH detected was 1,182,970 kb and 472,146 kb (Table 1). In addition, the data of < 1 Mb, 1–5 Mb, and > 5 Mb were counted according to the length of ROH. Among them, the FROH values of inbred individual were calculated, and the FROH < 1 Mb, FROH 1–5 Mb,

**Table 1** Statistics of ROH of inbred and non-inbred Amur tigers

| ROH lengths | Inbred | | | Non-inbred | | |
|---|---|---|---|---|---|---|
| | Number | Overall length (kb) | Length ratio (%) | Number | Overall length (kb) | Length ratio (%) |
| <1 Mb | 1292 | 417,139 | 35.26 | 675 | 193,778 | 41.04 |
| 1–5 Mb | 319 | 656,312 | 55.48 | 125 | 242,907 | 51.45 |
| > 5 Mb | 18 | 109,522 | 9.26 | 5 | 35,461 | 7.51 |
| Total | 1629 | 1,182,973 | — | 805 | 472,146 | — |

**Table 2** Inbreeding coefficient derived from ROHs with different lengths

| Sample | $F_{ROH < 1\ Mb}$ | $F_{ROH\ 1–5\ Mb}$ | $F_{ROH > 5\ Mb}$ | $F_{ROH > 1\ Mb}$ |
|---|---|---|---|---|
| Inbred | 0.174 | 0.274 | 0.046 | 0.319 |
| Non-inbred | 0.081 | 0.101 | 0.015 | 0.116 |

and FROH > 5 Mb were 0.174, 0.274, and 0.046, and the FROH values of non-inbred individual were 0.081, 0.101, and 0.015 (Table 2). Compared with non-inbred Amur tiger, inbred individuals had higher inbreeding coefficients in all length categories of ROH, and ROH in the 1–5 Mb length category contributed the most to the overall FROH. In order to evaluate the overall inbreeding level of Amur tigers, the FROH > 1 Mb of each individual was evaluated based on the total length of ROH (> 1 Mb). The results showed that the FROH > 1 Mb of non-inbred individual was 0.116, and that of inbred individual was 0.319, that is, compared with non-inbred, inbred Amur tiger had a higher inbreeding coefficient.

### Identification of heterogeneity in peripheral blood mononuclear cells between inbred and non-inbred Amur tigers

The collection and processing flow of peripheral blood samples from Amur tigers was illustrated in Fig. 1A; a total of 29,523 cells were harvested, delineating 19 distinct cell clusters (Fig. 1B). To characterize each cell cluster, we utilized well-established marker genes from the literature alongside cluster-specific marker genes, enabling us to accurately identify eight major cell types, mainly including B cells (CD79B, BANK1) [41], plasma (JCHAIN, MZB1) [41, 42], T cells (LEF1) [43], monocytes (CD14, VCAN) [44, 45], platelets (GP9), neutrophils (G0S2, CSF3R), classical dendritic cells type 2 (cDC2) (FCER1A), natural killer (NK) cells (GZMA, KLRD1) [46] (Fig. 1C). Following that, during the characterization of cells from the dataset comprising non-inbred individual and the combined dataset encompassing both inbred and non-inbred individuals, no discernible systematic differences were observed in the spatial distribution of distinct cell types within the UMAP plots (Fig. 1D, E). However, a lower proportion of B cells, cDC2 cells, NK cells, and T cells was observed in the inbred individual compared to the non-inbred individual (Fig. 1F). The statistical results of the number of each cell type are shown in Table 3.

### Subdivision and differential analysis of blood cell subpopulations in inbred and non-inbred individuals

#### *NK cell*

By conducting an unsupervised clustering analysis of 433 cells in the pooled dataset of inbred and non-inbred individuals, three distinct clusters were discerned and subsequently classified into two subpopulations, C1 and C2, according to specific gene expression signatures. Among them, the C1 subpopulation was characterized by distinctive expression of the *KLRB1* and *SELL* genes, while the C2 subpopulation exhibited specific expression of the *GZMH* gene (Fig. 2A). In analyzing differentially expressed genes and KEGG enrichment, we observed increased expression of genes, including *KLRB1*, *IKZF2*, and *SATB1* in the C1 subpopulation, while KEGG pathways associated with cgmp-pkg signaling pathways, pd-l1 expression and pd-1, and other regulatory pathways, were shown to be significantly enriched in this cluster (Fig. 2B, C left). The C2 subpopulation exhibited increased expression of cytotoxic genes, such as *GZMH* and *LOC102957957*, and KEGG analysis further revealed that this subgroup was markedly enriched in pathways associated with pathogenic escherichia coli infection and viral myocarditis (Fig. 2B, C right). Additionally, pseudotime analysis revealed that the C2 CD56dim NK cell subgroup originates from the C1 CD56bright NK cell subpopulation, aligning with the evolutionary trajectory of NK cell subgroups described in previous research [47] (Fig. 2D). Subsequent during the analysis of differentially expressed genes and KEGG enrichment in NK cells in the separate datasets of inbred and non-inbred individuals, we discovered that apart from showing heightened expression of cancer-associated genes, such as *PDE3B*, *RORA*, and *IQGAP2* (Fig. S1A), the findings revealed that NK cells from inbred individual were exhibited enriched in pathways including inflammatory mediator regulation of tpr channels, hepatitis b, and human cytomegalovirus infection (Fig. S1B).

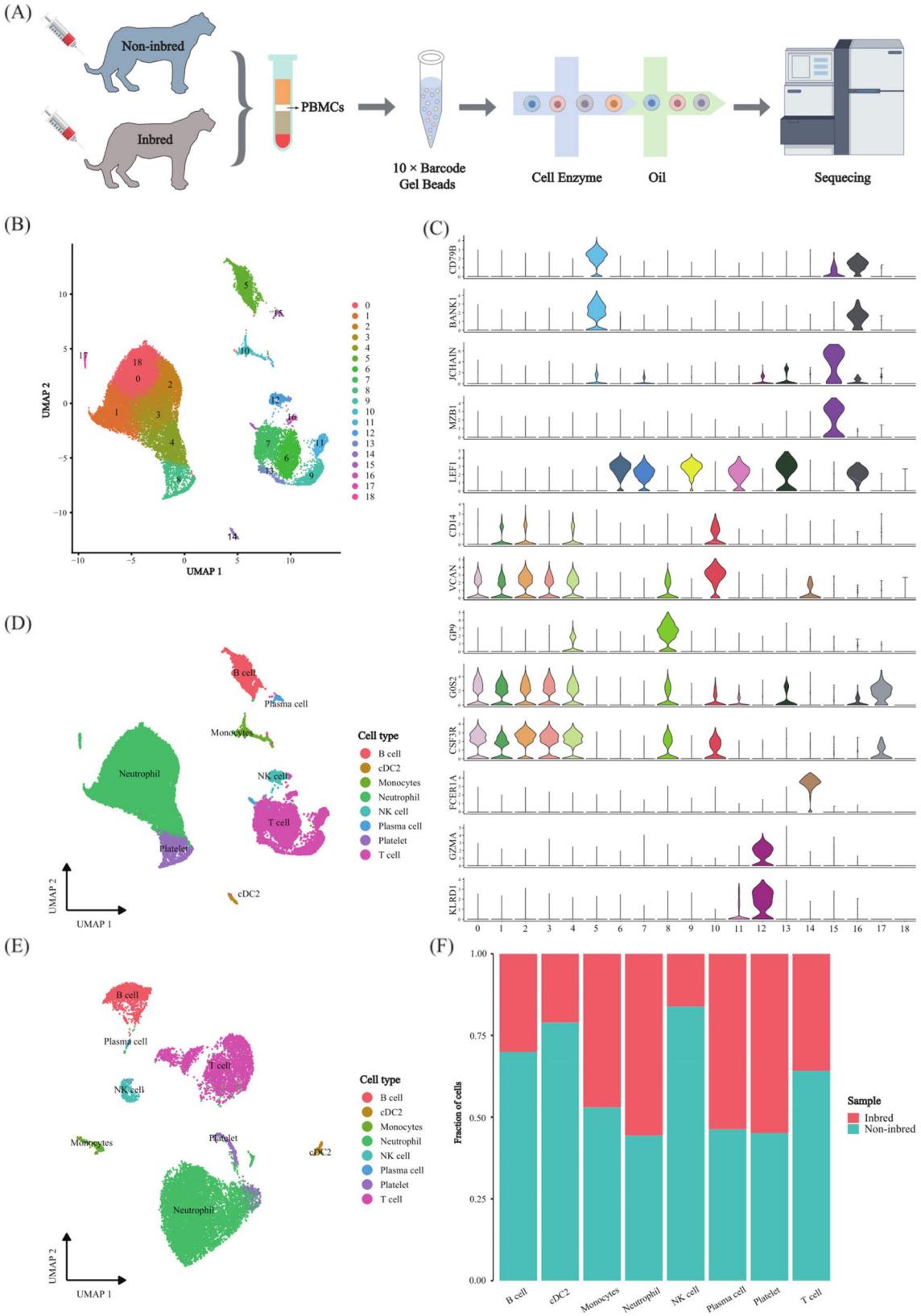


**Fig. 1** Single-cell gene expression profiles and cellular composition differences between inbred and non-inbred Amur tiger PBMCs. **A** Schematic diagram of the experimental workflow. **B** UMAP describes the outcomes of unsupervised clustering of 29,523 cells from the peripheral blood of two Amur tigers. **C** Violin maps of marker gene expression are utilized to characterize cell populations. **D** Cluster analysis of all cells, with each point representing a cell and colored based on cell type. **E** UMAP plot of non-inbred individual cell types. **F** Percentage of each cell type in inbred versus non-inbred individuals

**Table 3** Quantitative statistics of various cell types of inbred and non-inbred Amur tigers

| Cell type | Inbred | Non-inbred |
|---|---|---|
| B cell | 640 | 1488 |
| cDC2 | 51 | 191 |
| Monocytes | 232 | 261 |
| Neutrophil | 10802 | 8610 |
| NK cell | 70 | 363 |
| Plasma cell | 94 | 81 |
| Platelet | 655 | 539 |
| T cell | 1953 | 3493 |

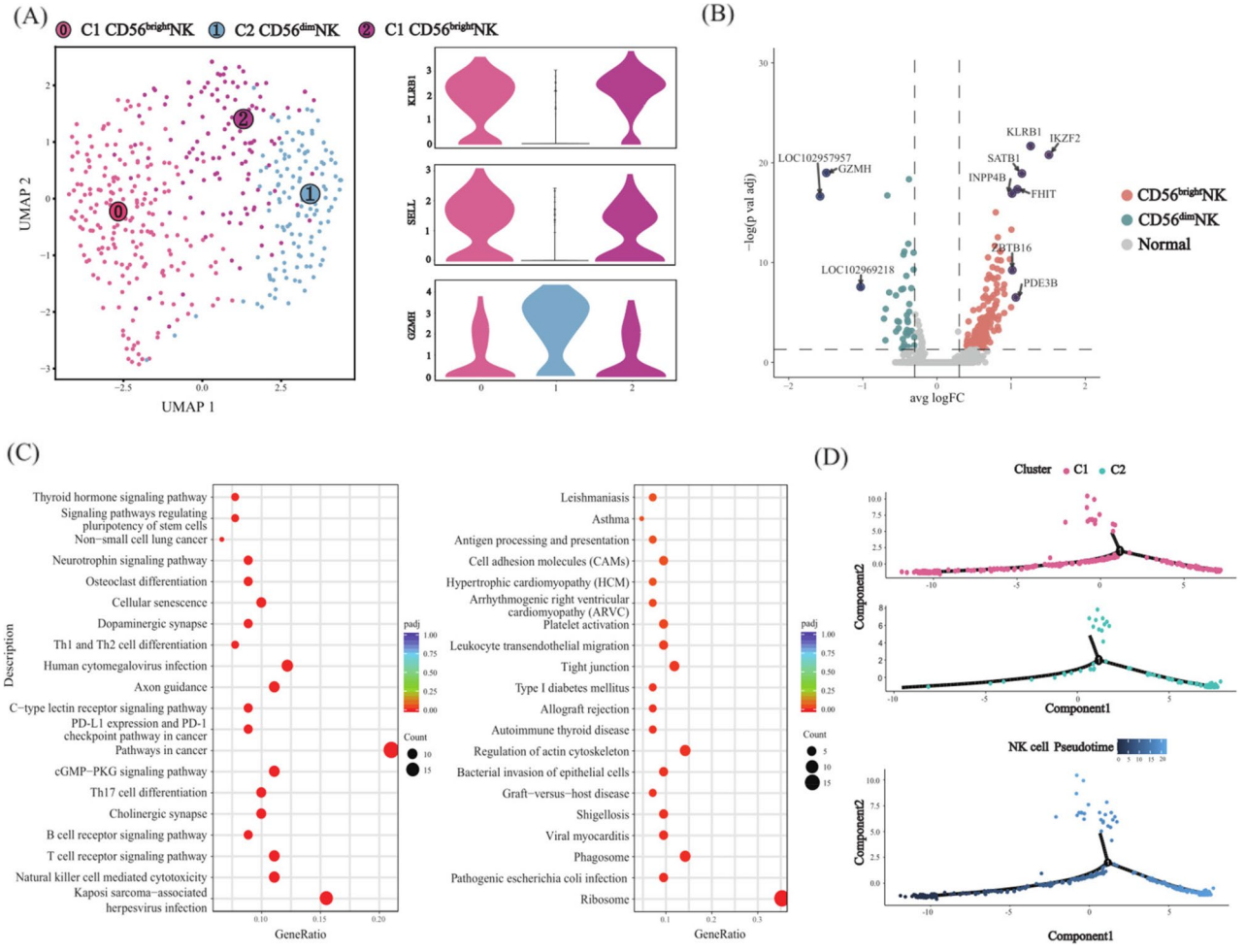


**Fig. 2** Division of NK cell subgroups in peripheral blood of the Amur tiger. **A** The unsupervised clustering results of 433 NK cells are depicted by UMAP on the left side; the violin diagram on the right depicts the typically expressed genes that constitute the natural killer cell subgroup. **B** The volcano map illustrates the differentially expressed genes found when CD56$^{bright}$NK cell clusters were compared to CD56$^{dim}$NK cell clusters. **C** KEGG enrichment results of differentially expressed genes in NK cell subsets showed CD56$^{bright}$NK cells on the left and CD56$^{dim}$NK cells on the right. **D** Results of pseudo-timing analysis of NK cell subsets

### *Monocyte*

The unsupervised clustering and subsequent subpopulation delineation of 493 cells in the pooled dataset yielded the discovery of five distinct clusters and three separate subpopulations. Expression of the genes *S100A8*, *CXCL8*, and *CD14* was uniquely observed in subpopulation C1, while genes *UST*, *CENPK*, *ADAMTS6*, and *LRMDA* exhibited specific expression in subpopulation C2 (Fig. 3A). The analysis of differential gene expression for each cluster revealed that the C1 subpopulation showed increased expression of the pro-inflammatory cytokine gene *IL18* [48], as well as the *S100A9* genes, which play crucial roles in regulating inflammatory processes and immune responses [49]. The C2 subpopulation

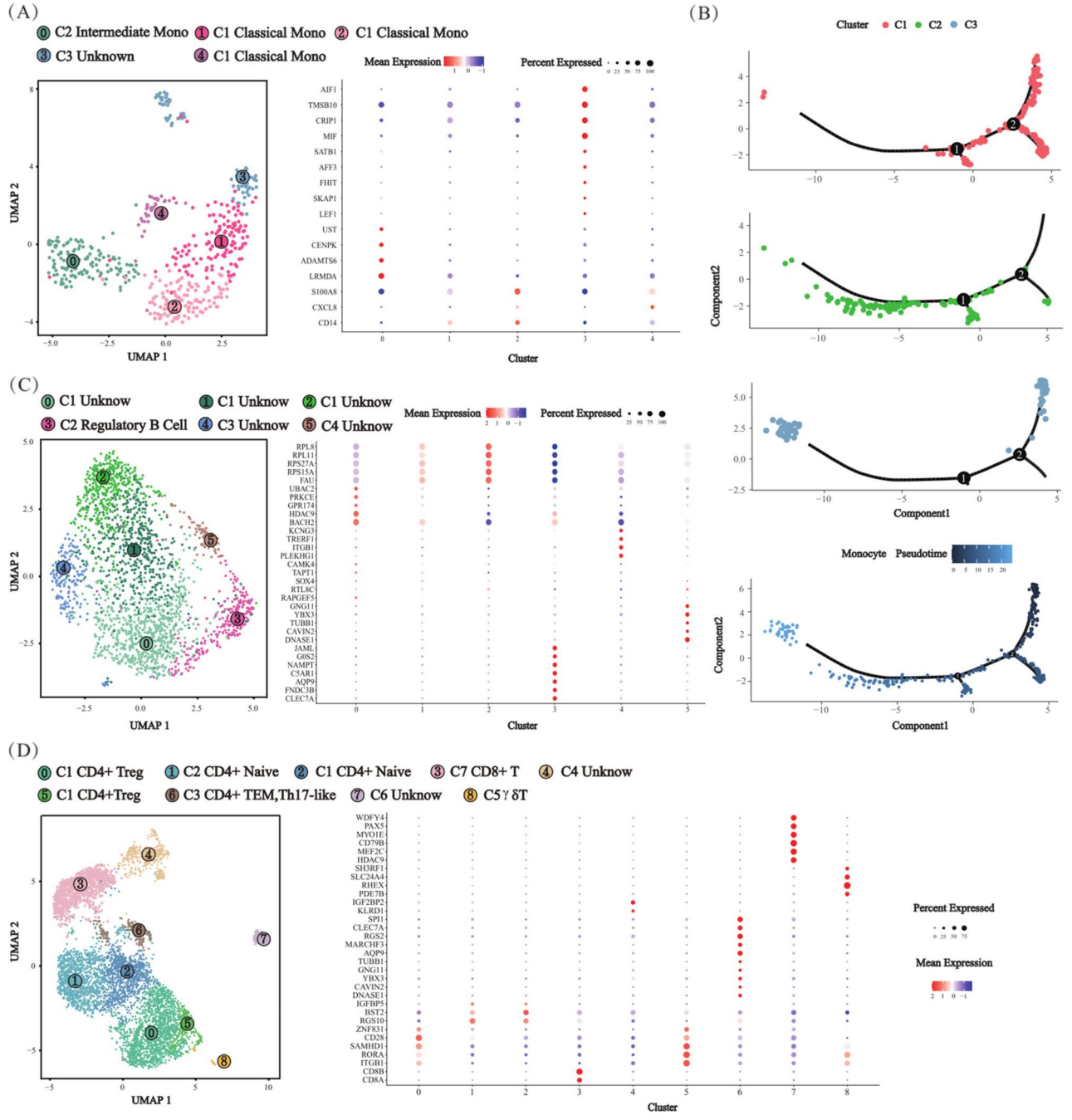


**Fig. 3** Peripheral blood mononuclear cells, B cells, and T cell subsets of the Amur tiger were divided. **A** UMAP on the left depicts the unsupervised clustering results of 493 monocytes; the right side is the characteristic expression gene point map for defining monocyte subsets. **B** Monocyte subsets'pseudotime analysis results. **C** On the left side is the UMAP diagram depicting the unsupervised clustering results of 2128 B cells; the typical expression gene dot map for distinguishing B cell subsets is shown on the right. **D** The UMAP visualization on the left shows the unsupervised clustering outcomes for 5446 T cells; the characteristic gene expression dot plot used to define T cell subsets is on the right

demonstrated elevated expression of *CD74* [50] and *LOC102961248* genes associated with antigen presentation (Fig. S2A). Furthermore, KEGG enrichment analysis revealed that the C1 subpopulation had a substantial enrichment in pathways such as the nod-like receptor signaling pathway, leukocyte transendothelial migration, and il-17 signaling pathway. Conversely, the C2 subpopulation demonstrated significant enrichment in the fc epsilon ri signaling pathway and the antigen processing and presentation (Fig. S2B). Consequently, the C1 and C2 subpopulations were identified as Classical Mono and Intermediate Mono, respectively. To validate the

accuracy of these subgroup classifications, we conducted pseudotime analysis, which confirmed that the C2 Intermediate Mono definitively originated from the C1 Classical Mono [51] (Fig. 3B).

During performing differential gene expression and KEGG enrichment analyses in monocytes in inbred and non-inbred separate datasets, pathways linked to hepatitis c, human cytomegalovirus infection, hepatitis b, and kaposi sarcoma-associated herpesvirus infection were significantly enriched in inbred individual (Fig. S5A).

#### *B cell and T cell*

The B cells in the pooled dataset, comprising a total of 2,128 cells, were classified into six clusters and further stratified into four distinct subpopulations. *RPL8*, *RPL11*, *RPS27A*, *RPS15A*, *FAU* and *BACH2* genes were unique expression in C1 subpopulation; subpopulation C2 specifically expressed *G0S2*, *NAMPT*, *C5AR1*, *AQP9*, *FNDC3B* and *CLEC7A* genes; subpopulation C3 displayed characteristic expression of *KCNG3*, *TRERF1*, *ITGB1*, and *PLEKHG*1genes; in subpopulation C4 specific expression was observed for the genes *GNG11*, *YBX3*, *TUBB1*, *CAVIN2*, and *DNASE1* (Fig. 3C). Nevertheless, compared to other subpopulations, the C2 subpopulation showed significant expression of the *S100A9* and *S100A8* genes, and previous studies have linked these genes to immune regulation, thus defining the C2 subpopulation as regulatory B cells (Fig. S3A). In addition, KEGG analysis findings provided additional evidence supporting the functional role of C2 as a regulatory B cell due to its high expression of immune-related pathways among various pathways, including the cytokine-cytokine receptor interaction [52] and il-17 signaling pathway [53] (Fig. S3B).

A total of 5,446 T cells were classified into seven subpopulations distributed across nine clusters. The C1 subpopulation exclusively expressed the genes *ZNF831*, *CD28*, *SAMHD1*, *RORA*, and *ITGB1*; *IGFBP5*, *BST2* and *RGS10* genes were particular expressed in C2 subpopulation; subpopulation C3 exhibited characteristic expression of the genes *SPI1*, *CLEC7A*, *RGS2*, *MARCHF3*, and *AQP9*; the genes *IGF2BP2*, and *KLRD1* were uniquely expressed in the C4 subpopulation; *SH3RF1*, *SLC24A4*, *RHEX*, and *PDE7B* were observed to be expressed in subpopulation C5; C6 subpopulation specifically expressed *WDFY4*, *PAX5*, *MYO1E*, *CD79B*, *MEF2C* and *HDAC9*; while particular expression of *CD8B* and *CD8A* was observed in subpopulation C7 (Fig. 3D). Subsequently, we carried out the characterization of cellular subpopulations based on the literature's uniquely expressed genes and marker genes; the C1, C2, and C7 subpopulations were identified as CD4 + Treg [54], CD4 + Naive [49], and CD8 + T [46] subtypes, respectively. Notably, the C3 subset exhibited significantly higher expression of inflammation-related genes such as *S100A8* and *S100A9* compared to all other subsets (Fig. S4A) [49]. Additionally, our KEGG analysis revealed a significant enrichment of the il-17 signaling pathway in this subset (Fig. S4B). Therefore, we defined the C3 subset as CD4 + TEM Th17-like. The C5 subset was designated as γδT cells due to its elevated expression of the gene *LOC102953909* (WC1.1 antigen) (Table S1), which is characterized as a marker for bovine γδT cells [55].

KEGG enrichment analysis was performed on B cells and T cells in the separate datasets of inbred and non-inbred individuals, respectively. We observed that B cells were significantly enriched in the following pathways: viral carcinogenesis, pathways in cancer, non-small cell lung cancer, kaposi sarcoma-associated herpesvirus infection, proteoglycans in cancer, human cytomegalovirus infection and hepatitis b. Moreover, significant enrichment in T cells was observed in the following pathways: human T-cell leukemia virus 1 infection, pathways in cancer, kaposi sarcoma-associated herpesvirus infection, non-small cell lung cancer, human cytomegalovirus infection and hepatitis b (Fig. S5A).

#### *Remaining cell types*

Ultimately, the transcriptomic differences among the remaining four cell types, namely cDC2, plasma cells, platelets, and neutrophils, were comprehensively analyzed in the separate datasets of inbred and non-inbred individuals. The findings revealed that cDC2 and plasma cells in inbred individual did not differ significantly at the pathway level compared to non-inbred individual. However, both platelets and neutrophils from inbred individual exhibited notable enrichment in human cytomegalovirus infection, pathways in cancer, and kaposi sarcoma-associated herpesvirus infection (Fig. S5B). Moreover, platelets demonstrated substantial enrichment in the proteoglycans in cancer, and neutrophils exhibited significant enrichment in the human immunodeficiency virus 1 infection (Fig. S5B).

### WGCNA analysis and identification of key genes

The WGCNA analysis discerned 13 gene modules based on the TOM matrix, with the MEblue module exhibiting a preliminary correlation with inbreeding status ($p = 0.05$) (Fig. 4A, B). Subsequently, we conducted KEGG enrichment analysis on the genes within the MEblue module, revealing potential associations with several cancer-related pathways, including hepatocellular carcinoma, erbb signaling pathway, hedgehog signaling pathway, thyroid cancer, and colorectal cancer (Fig. 4C). In this preliminary network, *YTHDC2* was identified as the top-ranking hub gene. Among the highest-scoring candidate genes were *KMT2A*, *COMMD10*, *MCM9*, *DHX15*, *MED27*, and *PARP14*, which have been previously associated with cancer in other species (Fig. 4D).

### Comparative global analysis of cell communication

The results obtained from the analysis of cell communication of separate datasets of inbred and non-inbred individuals revealed that the inbred individual exhibited 115 immune cell interactions, with a strength of 4.718, while the non-inbred individual displayed 95 interactions, with a strength of 5.198 (Fig. 4E, Fig. S6A). Moreover, inbred individual with demonstrated relatively higher inferred activity in the signaling pathways of TGFb, VISFATIN, APRIL, IL2, BAG, GRN, and IL16; conversely experiencing notable downregulation in the GALECTIN and CD40 signaling pathways (Fig. 4F, Fig. S6B). Simultaneously, we have identified nine pairs of specific ligand receptors exclusively present in inbred individual that play a crucial role in immune cell communication. These include NAMPT-(ITGA5 + ITGB1), NAMPT-INSR, TGFB1-(TGFBR1 + TGFBR2), TNFSF13-TNFRSF13B, TNFSF13-TNFRSF17, MIF-(CD74 + CXCR2), IL7-(IL7R+IL2RG), GRN-SORT1, and BAG6-NCR3 (Fig. 4G). Additionally, the MIF-(CD74 + CD44) interaction appeared stronger in the inbred individual.

## Discussion

Inbreeding enhances genetic homogeneity, which elevates the frequency of recessive deleterious alleles in a homozygous state and subsequently reduces the diversity and adaptability of the immune system [56]. However, at present, there is a critical knowledge gap exists in examining the immune heterogeneity of the moderately inbred Amur tiger. The emergence of single-cell RNA sequencing technology provides a promising avenue to rectify this deficiency through high-resolution data. Simultaneously, we contemplate the findings of Ammons et al. that age may lead to a reduction in canine immune cells [54]. Accordingly, this study concentrated on captive female Amur tigers aged one year to minimize potential age-related influences. We isolation of peripheral blood immune cells from whole blood samples of Amur tigers was followed by single-cell transcriptome analysis using the 10X genomics platform. This analysis aimed to map the peripheral blood immune cells of Amur tigers, elucidate the transcriptome features of various immune cell populations, and examine the immunological heterogeneity between inbred and non-inbred individuals.

### Cell types and proportion

With in this investigation, a total of eight principal cell types were delineated. Nevertheless, there were no apparent significant differences in the distribution of cell type between inbred and non-inbred individuals, nor were there any noticeable shifts in the localization of cell type across different samples. These findings suggest that inbreeding may not drastically alter the type and distribution of immune cells in blood. Notwithstanding, we observed a relative decrease in the proportions of cDC2 cells and lymphocytes in the inbred individual compared to non-inbred individual. Previous studies have shown that lower numbers of lymphocytes may affect the body's immune reaction, leading to a reduction in the body's ability to fight viruses. Moreover, zheng et al. noted a notable decline in NK cells and CD8 T cells in individuals infected with SARS-CoV-2 [57]; similarly, Cui et al. discovered a reduction in the absolute count of lymphocytes and the level of lymphocyte subsets in sepsis patients who experienced long-term immune decline, potentially resulting in an impaired ability to combat pathogens effectively [58]. Therefore, our findings raise the possibility that a similar lymphocytic deficit in inbred Amur tiger might contribute to diminished antiviral or overall immune capacity.

To achieve a more precise peripheral blood mononuclear cell atlas of the Amur tigers, we classified subgroups within NK cells, monocytes, B cells, and T cells. Based on established marker genes, specific expression genes, KEGG enrichment and validated pseudo-temporal analysis, we identified distinct cell subpopulations, including CD56bright NK (*SELL*+) [47]; CD56dim NK (*GZMH*+) [59]; Classical Mono (*IL18*+, *S100A9*+); Intermediate Mono (*CD74*+); Regulatory B (*C5AR1*+, *S100A8*+, *S100A9*+); CD4 + Treg (*CD28*+, *ZNF831*+); CD4 + Naive (*RGS10*+); CD4 + TEM, Th17-like (*S100A8*+, *S100A9*+) [54]; CD8 + T (*CD8A*+, *CD8B*+) [60]; γδT (*LOC102953909*) [55].

### KEGG enrichment analysis of different cell types

Beyond that, the results of KEGG enrichment analysis of each cell type in the separate datasets of inbred and non-inbred individuals showed that associations of inbred individual with virus infections, inflammation, and cancer-related pathways, as demonstrated by human cytomegalovirus infection, kaposi sarcoma-associated herpesvirus infection, hepatitis b, and pathways in cancer. Of these, human cytomegalovirus infection occurs primarily in people with weakened immune systems [61], and in addition, the virus' DNA has been found in malignant tissues from patients with prostate [62], colorectal [63], and glioblastoma cancers [64]. Moreover, numerous studies have demonstrated that the virus can induce transformation and carcinogenesis in glioblastoma cells and other cell types in vitro, establishing a link between human cytomegalovirus infection and the proliferation of cancerous cells [65, 66]. Additionally, kaposi sarcoma-associated herpesvirus is an infectious etiology of various types of KS tumors and an oncogenic gamma herpesvirus [67] that is frequently detected in HIV-positive cancer patients who are not receiving treatment [68, 69]. Meanwhile, hepatitis b is a severe liver infection caused by the hepatitis b virus (HBV), which significantly contributes

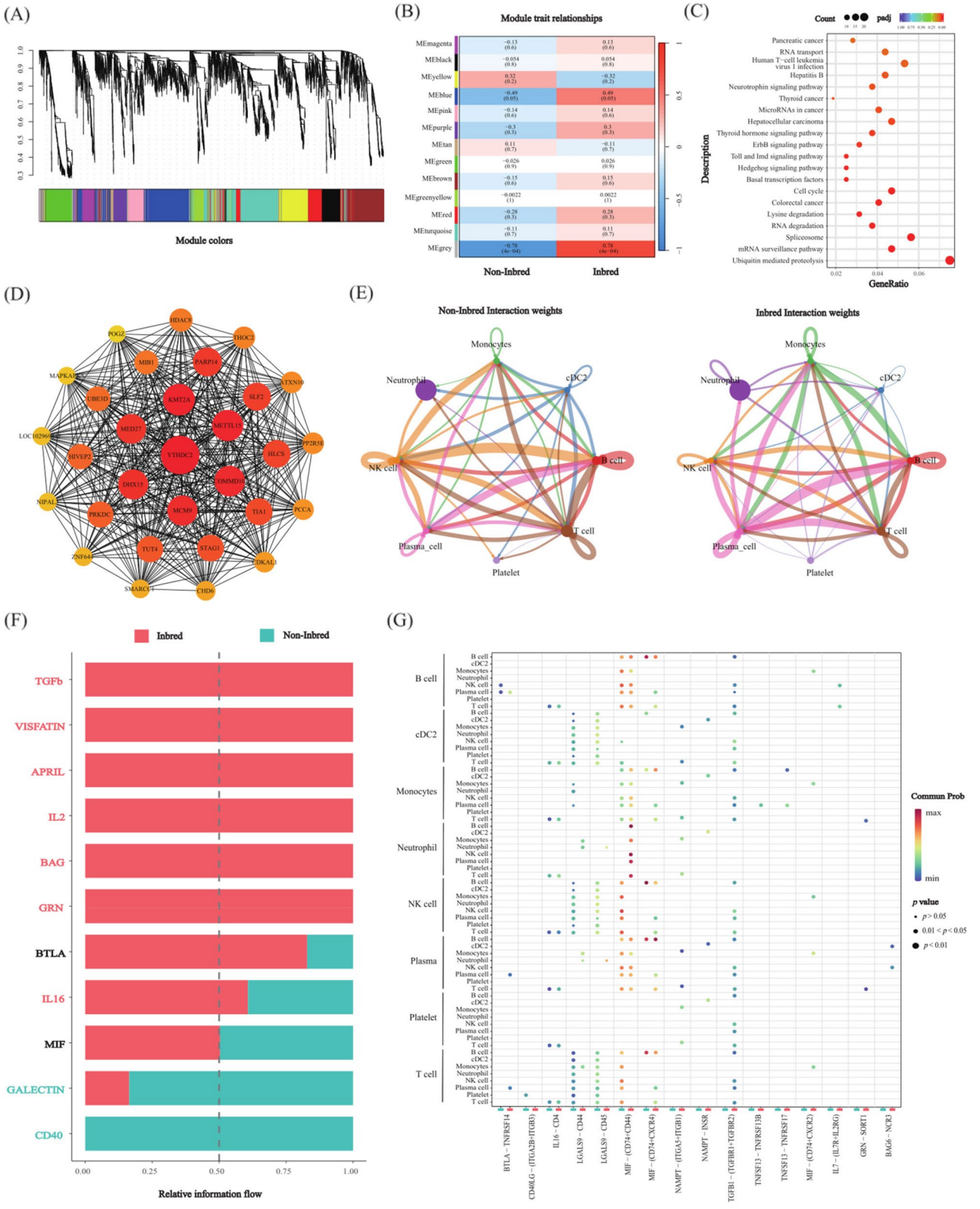


**Fig. 4** (See legend on next page.)

(See figure on previous page.)

**Fig. 4** WGCNA study of peripheral blood cells and differential in contacts between cells of inbred and non-inbred individuals in Amur tigers. **A** A total of 13 gene co-expression modules were identified through the dendrogram of co-expression module clustering. **B** Heatmap of module trait relationships, with blue modules most associated with inbred individuals. **C** Results of KEGG enrichment analysis of genes within the blue module. **D** Blue module gene co-expression network in the scores of the top 30 nodes of the network, the darker the color the higher the score. **E** Plot of the strength of cellular communication between non-inbred and inbred individuals. **F** Bar charts showing significant signaling pathways ranked according to the difference in overall information flow between inbred and non-inbred intersections in the inferred network. The apical signaling pathway colored red is enriched in inbred individuals and the apical signaling pathway colored light blue is enriched in non-inbred individuals. The black signal pathway is not significant in both. **G** Dot plot of predicted interactions between inbred and non-inbred immune cell types, the p-value is represented by the size of the dot. The mean value of the average expression level of the interaction of each group of ligand pairs is represented by color

to cirrhosis and liver cancer globally [70]. However, it should be recognized that, given only one sample per condition, the observed enrichment of these pathways in the inbred individual might reflect individual biological variability rather than a conclusive inbreeding effect. Combined with the existing literature, these preliminary results suggest the possibility that inbred Amur tiger may experience immune alterations that could make them more susceptible to viruses, chronic inflammation, and, in the long run, an increased oncogenic risk.

#### Screening of key genes in inbred individual

The WGCNA approach enables the identification of gene correlation and differentially expressed genes between groups [71]. In this study, the MEblue module was identified as significantly enriched in inbred individual, particularly in cancer pathways, with thyroid cancer being specifically associated with inbreeding. Thomsen et al. identified significantly higher inbreeding coefficients in thyroid cancer patients compared to controls based on genome-wide association studies data [72]. Similarly, Dutch German longhaired pointers with thyroid follicular cell cancer exhibited an inbreeding coefficient reached 0.25 [73]. Furthermore, a substantial enrichment of the MEblue module was observed in the hedgehog signaling pathway, which is intricately associated with elevated cancer incidence, malignant development, unfavorable prognosis, and even greater death rates [74]. Simultaneously, in evidence-based medicine, the hedgehog signaling pathway is acknowledged as a crucial catalyst for cancer and malignancy when it deviates from regular expression [75]. Additionally, the MEblue module was also notably enriched in the erbb signaling pathway, where the overactivation or abnormal expression of receptors within the erbb family can result in unchecked cell growth, ultimately leading to cancer development [76]. In the gene interaction network diagram, *YTHDC2* exhibits the most significant score in the MEblue module of this investigation. In addition, previous studies have shown that it is not only linked to the advancement of cancer in breast and colorectal malignancies [77, 78] but also increased in radiation-resistant nasopharyngeal carcinoma, hepatocellular carcinoma, glioblastoma, and prostate cancer tumors [79–83]. Besides, Yuan et al. identified *YTHDC2* as a novel oncogene in gastric cancer through investigation utilizing the xenograft tumor model [84]. Meanwhile, beyond *YTHDC2*, six additional genes (*KMT2A* [85, 86], *COMMD10* [87], *MCM9* [88], *DHX15* [89], *MED27* [90], *PARP14* [91]) ranked among the top ten in the scores exhibit significant expression patterns across various cancer types including breast, colorectal, liver, and gastric cancers. Among these genes, aberrant localization of *KMT2A* can result in a potent cancer-causing gene leading to highly aggressive acute leukemias [92], *DHX15* may be an oncogenic gene in the development of Burkitt's lymphoma [93], and *MED27* gene has been shown to play an oncogenic role in breast and stomach cancer [94]. Collectively, these analyses indicate an enrichment of cancer and inflammation-related pathways and genes in inbred Amur tiger. Nevertheless, it is crucial to note that given the limited sample size ($n$ = 1 per condition in this study), the observed disparities in module enrichment and gene expression might reflect individual biological variability rather than a consistent impact of inbreeding.

#### Differences in cell communication between inbred and non-inbred individuals

Efficient intercellular communication serves as an indicator of immune system homeostasis, with extreme variations in cell signaling strength potentially indicating immune dysregulation [95, 96]. By employing CellChat analysis, Huang et al. revealed that patients with Parkinson's disease exhibited a reduction in overall communication volume accompanied by amplification in intensity, positing that the elevated intensity could offset the diminished quantity to reestablish physiological equilibrium [97]. Nevertheless, our results revealed that inbred individual exhibited an increased number of immune cell connections and a simultaneous reduction in the strength of these interactions. Based on the observed results, we conjecture that the immune system in inbred individual may be in a heightened state of activation, potentially as a response to persistent infections or underlying disease processes. This may lead to an increased recruitment of immune cells, and disease associated cells may engage mechanisms such as the expression of immune checkpoint proteins or the secretion of immune suppressive factors, which could dampen specific aspects of intercellular communication [98, 99]. Signaling pathways that

were altered in inbred individual also indicated that it had an altered immune reaction. In the highly increased immune cell interaction route of individuals with inbred, the TGFb signaling pathway plays a crucial role in triggering tumor EndMT (Endothelial-to-Mesenchymal Transition), and it has been shown in several types of cancer, including melanoma, esophageal cancer, colon cancer, and lung cancer [100–103]. Elevated levels of TGFb can impact the immune response and alter the tumor microenvironment, potentially facilitating disease progression [104]. Moreover, VISFATIN a pro-inflammatory cytokine, serves as a serum biomarker and prognostic factor for endometrial cancer [105]. Recently, Shi et al. discovered that the interaction between Nampt-Insr and Nampt-Itga5 / Itgb1 axis was strengthened in the VISFATIN/Nampt signal transduction in mice infected with chronic hepatitis B virus [106]. At the same time, VISFATIN and TGFb were found to be strongly associated with EndMT, potentially facilitating glioma angiogenesis through the promotion of the EndMT process [107].

Besides, APRIL (TNFSF13) is a constituent of the pro-inflammatory and pro-apoptotic mediator TNF [108] and serves as a functional element for lymphatic malignancies and immuno-related disorders, which can facilitate tumor proliferation and induce apoptosis [109]. Through its interaction with TACI (TNFRSF13B), APRIL has the potential to either preserve or improve the survival of leukemia cells, influencing the course of the illness and the prognosis of patients [110]. Concurrently, the interactions between the APRIL and BCMA (TNFRSF17) axis are enhanced in hepatocellular carcinoma compared to normal liver tissue [111]. Furthermore, this study found a significant enhancement of the MIF-(CD74 + CD44) axis in inbred individual; MIF promoted the binding of CD44 to CD74 by increasing the expression of CD44 in cells, forming a signal transduction complex, resulting in the production of different splicing forms of CD44 v3/v6 associated with tumors [112]. Therefore, the heightened activity of pro-inflammatory and pro-cancer signaling pathways observed in inbred individual implies that it might be linked to the activation of inflammatory responses and cell damage processes. And the persistent activation of relevant signaling pathways might be further implicated in the establishment of chronic inflammatory states, thereby theoretically creating a microenvironment conducive to cancer development.

At the same time, the signaling pathways of both CD40 and GALECTIN, which govern anti-tumor and immunological activities, exhibited downregulation in inbred individual. Activation of CD40 stimulates fatty acid oxidation (FAO) and glutamine metabolism, leading to ATP citrate lyase-dependent epigenetic reprogramming, which enhances the anti-tumor effects on macrophages [113]; GALECTIN can impact immunological activity and regulate both innate and adaptive immune cells through its interaction with glycans on the surface of immune cells [114]. Consequently, we believe that inbred individual may have a tendency to exhibit decreased immune response activity and impaired anti-tumor function, thus facing a higher risk of dysregulated inflammation and tumor development.

#### Limitations and prospects

The immune heterogeneity between inbred and non-inbred individuals was investigated using single-cell transcriptome technology in this study. The findings revealed that inbreeding exerts a detrimental impact on the immune system of the Amur tiger, which may increase the risk of inflammation and cancer in their offspring. However, there are still some limitations in this study. Firstly, in terms of sample selection, in order to control variable interference, we only included captive Amur tigers with different degrees of inbreeding that matched age and gender and had no history of antibiotic use in the past three months. Nevertheless, the number of captive individuals that met the above conditions was extremely limited, resulting in a small final sample size and insufficient biological repetition, which may affect the robustness and universality of the statistical results. Secondly, although single-cell transcriptome sequencing and WGCNA analysis jointly suggest that the *YTHDC2* gene plays a central role in inbreeding-related carcinogenic pathways, this study has not yet verified the functional level of the gene. The specific mechanism of *YTHDC2* in the immune regulation and tumorigenesis of the Amur tiger remains to be further explored. In addition, this study mainly focused on the transcriptome characteristics at the PBMC level and failed to integrate the data at the proteome or epigenetic level. Therefore, there is a certain gap in the association between gene expression and functional phenotype. At the same time, due to the differences between the captive environment and wild habitat, the potential effects of external factors such as diet, space, and behavior management on gene expression and inflammatory response have not been included in the analysis, which may limit the extrapolation of research conclusions to some extent. Accordingly, on the basis of expanding the sample size, future research should combine experimental methods such as gene knockout and overexpression to explore the functional mechanism of key genes and pathways affected by inbreeding in tumorigenesis, and further consider the impact of environmental variables on the health of Amur tigers.

In conclusion, we investigated the immune heterogeneity between inbred and non-inbred individuals, focusing on cell quantity, gene expression levels, and pathway analysis. This work provides a database for finding effective ways to treat inbred Amur tiger diseases, contributes

to the healthy development of wild Amur tiger populations, and provides a new direction for research on other inbred wildlife in order to achieve harmonious development of ecosystems.

## Supplementary Information

The online version contains supplementary material available at https://doi.org/10.1186/s12864-026-12872-y.

Supplementary Material 1.

**Acknowledgements**
We thank Changchun Zoological and Botanical Park and Baoshanqian Wild Animal Park for their support.

**Authors' contributions**
J.B., X.H. conducted data analysis and wrote the manuscript. D.M., C.L., W.K., Y.Y., D.J., J.L. and Y.Z. conducted field sample collection. Y.N. conceived the review and revised the manuscript. All authors reviewed and approved the final manuscript.

**Funding**
This research was supported by the following grant: National Natural Science Foundation of China (NSFC 32470547, NSFC 32100403).

**Data availability**
The data generated in this study have been deposited in public repositories. The whole genome sequencing data (Project: PRJNA1443692) are available in the Sequence Read Archive (SRA) of NCBI. The single-cell RNA sequencing data (Project: E-MTAB-15936) are available in the ArrayExpress database at EMBL-EBI.

## Declarations

**Ethics approval and consent to participate**
All samples were collected with the informed consent of the owners, and the collection process was approved by the Laboratory Animal Welfare and Ethics Committee of Jilin Agricultural University.

**Consent for publication**
Not applicable.

**Competing interests**
The authors declare no competing interests.

Received: 14 October 2025 / Accepted: 15 April 2026
Published online: 25 April 2026

**References**

1. Yuan R, Zhang N, Zhang Q. The impact of habitat loss and fragmentation on biodiversity in global protected areas. Sci Total Environ. 2024;931:173004. https://doi.org/10.1016/j.scitotenv.2024.173004.
2. Fox CW. Problems in measuring among-family variation in inbreeding depression. Am J Bot. 2005;92(11):1929–32. https://doi.org/10.3732/ajb.92.11.1929.
3. Naji MM, Gualdrón Duarte JL, Forneris NS, Druet T. Inbreeding depression is associated with recent homozygous-by-descent segments in Belgian Blue beef cattle. Genet Sel Evol. 2024;56(1):10. https://doi.org/10.1186/s12711-024-00878-7.
4. Frankham R, Ballou JD, Ralls K, Eldridge MDB, Dudash MR, Fenster CB et al. Inbreeding reduces reproductive fitness. Genetic Management of Fragmented Animal and Plant Populations. 2017;3:41–64. https://doi.org/10.1093/oso/9780198783398.003.0003.
5. Reid JM, Arcese P, Keller LF, Elliott KH, Sampson L, Hasselquist D. Inbreeding effects on immune response in free-living song sparrows (*Melospiza melodia*). Proc Biol Sci. 2007;274(1610):697–706. https://doi.org/10.1098/rspb.2006.0092.
6. Talal N. Immune Response Disorders. Acad Press. 1983;17:391–9. https://doi.org/10.1016/B978-0-12-262503-9.50024-4.
7. Shultz CL, Badowski M, Harris DT. The Immune Response in Inbred and Outbred Strains of Mice before and after Bone Marrow Transplantation. Libertas academica. 2013;2013:9–18. https://doi.org/10.1128/iai.54.2.522-528.1986.
8. Townsend AK, Taff CC, Wheeler SS, Weis AM, Hinton MG, Jones ML, et al. Low heterozygosity is associated with vector-borne disease in crows. Ecosphere. 2018;9:e02407. https://doi.org/10.1002/ecs2.2407.
9. Reid JM, Arcese P, Keller LF. Inbreeding depresses immune response in song sparrows (*Melospiza melodia*): direct and inter-generational effects. Proc Biol Sci. 2003;270(1529):2151–7. https://doi.org/10.1098/rspb.2003.2480.
10. Kwak K, Akkaya M, Pierce SK. B cell signaling in context. Nat Immunol. 2019;20(8):963–9. https://doi.org/10.1038/s41590-019-0427-9.
11. Liu J, Zhang X, Cheng Y, Cao X. Dendritic cell migration in inflammation and immunity. Cell Mol Immunol. 2021;18(11):2461–71. https://doi.org/10.1038/s41423-021-00726-4.
12. Říhová-Skárová B, Říha I. Host genotype and antibody formation. Curr Top Microbiol Immunol. 1972;57:159–87.
13. Spielman D, Brook BW, Briscoe DA, Frankham R. Does inbreeding and loss of genetic diversity decrease disease resistance. Conserv Genet. 2004;5:439–48. https://doi.org/10.1023/B:COGE.0000041030.76598.cd.
14. Ujvari B, Klaassen M, Raven N, Russell T, Vittecoq M, Hamede R, et al. Genetic diversity, inbreeding and cancer. Proc Biol Sci. 2018;285(1875):20172589. https://doi.org/10.1098/rspb.2017.2589.
15. Wen L, Tang F. Recent advances in single-cell sequencing technologies. Precis Clin Med. 2022;5(1):pbac002. https://doi.org/10.1093/pcmedi/pbac002.
16. Kashima Y, Suzuki A, Suzuki Y. An informative approach to single-cell sequencing analysis. Adv Exp Med Biol. 2019;1129:81–96. https://doi.org/10.1007/978-981-13-6037-4_6.
17. Ning Y, Kostyria AV, Ma J, Chayka MI, Guskov VY, Qi J, et al. Dispersal of Amur tiger from spatial distribution and genetics within the eastern Changbai mountain of China. Ecol Evol. 2019;9(5):2415–24. https://doi.org/10.1002/ece3.4832.
18. Wang D, Smith JLD, Accatino F, Ge J, Wang T. Addressing the impact of canine distemper spreading on an isolated tiger population in northeast Asia. Integr Zool. 2023;18(6):994–1008. https://doi.org/10.1111/1749-4877.12712.
19. Ning Y, Liu D, Gu J, Zhang Y, Roberts NJ, Guskov VY, et al. The genetic status and rescue measure for a geographically isolated population of Amur tigers. Sci Rep. 2024;14(1):8088. https://doi.org/10.1038/s41598-024-58746-9.
20. Ning Y, Roberts NJ, Qi J, Peng Z, Long Z, Zhou S, et al. Inbreeding status and implications for Amur tigers. Anim Conserv. 2021;25:521–31. https://doi.org/10.1111/acv.12761.
21. Chen S, Zhou Y, Chen Y, Gu J. fastp: an ultra-fast all-in-one FASTQ preprocessor. Bioinformatics. 2018;34(17):i884–90. https://doi.org/10.1093/bioinformatics/bty560.
22. Li H, Durbin R. Fast and accurate short read alignment with Burrows-Wheeler transform. Bioinformatics. 2009;25(14):1754–60. https://doi.org/10.1093/bioinformatics/btp324.
23. Li H. A statistical framework for SNP calling, mutation discovery, association mapping and population genetical parameter estimation from sequencing data. Bioinformatics. 2011;27(21):2987–93. https://doi.org/10.1093/bioinformatics/btr509.
24. Wang K, Li M, Hakonarson H. ANNOVAR: functional annotation of genetic variants from high-throughput sequencing data. Nucleic Acids Res. 2010;38(16):e164. https://doi.org/10.1093/nar/gkq603.
25. McQuillan R, Leutenegger AL, Abdel-Rahman R, Franklin CS, Pericic M, Barac-Lauc L, et al. Runs of homozygosity in European populations. Am J Hum Genet. 2008;83(3):359–72. https://doi.org/10.1016/j.ajhg.2008.08.007.
26. Kamath T, Abdulraouf A, Burris SJ, Langlieb J, Gazestani V, Nadaf NM, et al. Single-cell genomic profiling of human dopamine neurons identifies a population that selectively degenerates in Parkinson's disease. Nat Neurosci. 2022;25(5):588–95. https://doi.org/10.1038/s41593-022-01061-1.
27. Satija R, Farrell JA, Gennert D, Schier AF, Regev A. Spatial reconstruction of single-cell gene expression data. Nat Biotechnol. 2015;33(5):495–502. https://doi.org/10.1038/nbt.3192.
28. Butler A, Hoffman P, Smibert P, Papalexi E, Satija R. Integrating single-cell transcriptomic data across different conditions, technologies, and species. Nat Biotechnol. 2018;36(5):411–20. https://doi.org/10.1038/nbt.4096.

29. Robinson MD, McCarthy DJ, Smyth GK. edgeR: a Bioconductor package for differential expression analysis of digital gene expression data. Bioinformatics. 2010;26(1):139–40. https://doi.org/10.1093/bioinformatics/btp616.
30. Ashburner M, Ball CA, Blake JA, Botstein D, Butler H, Cherry JM, et al. Gene ontology: tool for the unification of biology. The Gene Ontology Consortium. Nat Genet. 2000;25(1):25–9. https://doi.org/10.1038/75556.
31. Kanehisa M, Araki M, Goto S, Hattori M, Hirakawa M, Itoh M, et al. KEGG for linking genomes to life and the environment. Nucleic Acids Res. 2008;36:D480–4. https://doi.org/10.1093/nar/gkm882.
32. Yu G, Wang LG, Han Y, He QY. clusterProfiler: an R package for comparing biological themes among gene clusters. OMICS. 2012;16(5):284–7. https://doi.org/10.1089/omi.2011.0118.
33. Haynes W. Benjamini–Hochberg method. Encyclopedia of Systems Biology. New York. 2013. https://doi.org/10.1007/978-1-4419-9863-7_1215.
34. Qiu X, Mao Q, Tang Y, Wang L, Chawla R, Pliner HA, et al. Reversed graph embedding resolves complex single-cell trajectories. Nat Methods. 2017;14(10):979–82. https://doi.org/10.1038/nmeth.4402.
35. Langfelder P, Horvath S. WGCNA: an R package for weighted correlation network analysis. BMC Bioinformatics. 2008;9:559. https://doi.org/10.1186/1471-2105-9-559.
36. Morandin C, Tin MM, Abril S, Gómez C, Pontieri L, Schiøtt M, et al. Comparative transcriptomics reveals the conserved building blocks involved in parallel evolution of diverse phenotypic traits in ants. Genome Biol. 2016;17:43. https://doi.org/10.1186/s13059-016-0902-7.
37. Cao L, Chen Y, Zhang M, Xu DQ, Liu Y, Liu T, et al. Identification of hub genes and potential molecular mechanisms in gastric cancer by integrated bioinformatics analysis. PeerJ. 2018;6:e5180. https://doi.org/10.7717/peerj.5180.
38. Chin CH, Chen SH, Wu HH, Ho CW, Ko MT, Lin CY. cytoHubba: identifying hub objects and sub-networks from complex interactome. BMC Syst Biol. 2014;8(Suppl 4):S11. https://doi.org/10.1186/1752-0509-8-S4-S11.
39. Lagger C, Ursu E, Equey A, Avelar RA, Pisco AO, Tacutu R, et al. scDiffCom: a tool for differential analysis of cell-cell interactions provides a mouse atlas of aging changes in intercellular communication. Nat Aging. 2023;3(11):1446–61. https://doi.org/10.1038/s43587-023-00514-x.
40. Jin S, Guerrero-Juarez CF, Zhang L, Chang I, Ramos R, Kuan CH, et al. Inference and analysis of cell-cell communication using CellChat. Nat Commun. 2021;12(1):1088. https://doi.org/10.1038/s41467-021-21246-9.
41. Lyu M, Shi X, Liu Y, Zhao H, Yuan Y, Xie R, et al. Single-Cell Transcriptome Analysis of H5N1-HA-Stimulated Alpaca PBMCs. Biomolecules. 2022;13(1):60. https://doi.org/10.3390/biom13010060.
42. Zhu H, Chen J, Liu K, Gao L, Wu H, Ma L, et al. Human PBMC scRNA-seq-based aging clocks reveal ribosome to inflammation balance as a single-cell aging hallmark and super longevity. Sci Adv. 2023;9(26):eabq7599. https://doi.org/10.1126/sciadv.abq7599.
43. Luo T, Zheng F, Wang K, Xu Y, Xu H, Shen W, et al. A single-cell map for the transcriptomic signatures of peripheral blood mononuclear cells in end-stage renal disease. Nephrol Dial Transpl. 2021;36(4):599–608. https://doi.org/10.1093/ndt/gfz227.
44. Qu HQ, Kao C, Garifallou J, Wang F, Snyder J, Slater DJ, et al. Single Cell Transcriptome Analysis of Peripheral Blood Mononuclear Cells in Freshly Isolated versus Stored Blood Samples. Genes. 2023;14(1):142. https://doi.org/10.3390/genes14010142.
45. Song W, Wang G, Wang C, Liu L, Zhang L, Zhang R, et al. Case Report: An unclassified T cell lymphoma subtype with co-expression of TCR αβ and γ chains revealed by single cell sequencing. Front Immunol. 2023;14:1184383. https://doi.org/10.3389/fimmu.2023.1184383.
46. Mo L, Yu Z, Lv Y, Cheng J, Yan H, Lu W, et al. Single-Cell RNA Sequencing of Metastatic Testicular Seminoma Reveals the Cellular and Molecular Characteristics of Metastatic Cell Lineage. Front Oncol. 2022;12:871489. https://doi.org/10.3389/fonc.2022.871489.
47. Yang C, Siebert JR, Burns R, Gerbec ZJ, Bonacci B, Rymaszewski A, et al. Heterogeneity of human bone marrow and blood natural killer cells defined by single-cell transcriptome. Nat Commun. 2019;10(1):3931. https://doi.org/10.1038/s41467-019-11947-7.
48. Yamanishi K, Doe N, Mukai K, Hashimoto T, Gamachi N, Hata M, et al. Acute stress induces severe neural inflammation and overactivation of glucocorticoid signaling in interleukin-18-deficient mice. Transl Psychiatry. 2022;12(1):404. https://doi.org/10.1038/s41398-022-02175-7.
49. Gebhardt C, Németh J, Angel P, Hess J. S100A8 and S100A9 in inflammation and cancer. Biochem Pharmacol. 2006;72(11):1622–31. https://doi.org/10.1016/j.bcp.2006.05.017.
50. Basha G, Omilusik K, Chavez-Steenbock A, Reinicke AT, Lack N, Choi KB, et al. A CD74-dependent MHC class I endolysosomal cross-presentation pathway. Nat Immunol. 2012;13(3):237–45. https://doi.org/10.1038/ni.2225.
51. Patel AA, Zhang Y, Fullerton JN, Boelen L, Rongvaux A, Maini AA, et al. The fate and lifespan of human monocyte subsets in steady state and systemic inflammation. J Exp Med. 2017;214(7):1913–23. https://doi.org/10.1084/jem.20170355.
52. Kim S, Lim B, Mattoo SU, Oh EY, Jeong CG, Kim WI, et al. Comprehensive Transcriptomic Comparison between Porcine CD8- and CD8 + Gamma Delta T Cells Revealed Distinct Immune Phenotype. Animals. 2021;11(8):2165. https://doi.org/10.3390/ani11082165.
53. Jiang K, Xu Y, Wang Y, Yin N, Huang F, Chen M. Unveiling the role of IL-17: Therapeutic insights and cardiovascular implications. Cytokine Growth Factor Rev. 2024;77:91–103. https://doi.org/10.1016/j.cytogfr.2024.05.001.
54. Ammons DT, Harris RA, Hopkins LS, Kurihara J, Weishaar K, Dow S. A single-cell RNA sequencing atlas of circulating leukocytes from healthy and osteosarcoma affected dogs. Front Immunol. 2023;14:1162700. https://doi.org/10.3389/fimmu.2023.1162700.
55. Bhat SA, Elnaggar M, Hall TJ, McHugo GP, Reid C, MacHugh DE, et al. Preferential differential gene expression within the WC1.1 + γδ T cell compartment in cattle naturally infected with *Mycobacterium bovis*. Front Immunol. 2023;14:1265038. https://doi.org/10.3389/fimmu.2023.1265038.
56. Charlesworth D, Willis JH. The genetics of inbreeding depression. Nat Rev Genet. 2009;10(11):783–96. https://doi.org/10.1038/nrg2664.
57. Zheng M, Gao Y, Wang G, Song G, Liu S, Sun D, et al. Functional exhaustion of antiviral lymphocytes in COVID-19 patients. Cell Mol Immunol. 2020;17(5):533–5. https://doi.org/10.1038/s41423-020-0402-2.
58. Cui Z, Wang L, Li H, Feng M. Study on immune status alterations in patients with sepsis. Int Immunopharmacol. 2023;118:110048. https://doi.org/10.1016/j.intimp.2023.110048.
59. Crinier A, Milpied P, Escalière B, Piperoglou C, Galluso J, Balsamo A, et al. High-Dimensional Single-Cell Analysis Identifies Organ-Specific Signatures and Conserved NK Cell Subsets in Humans and Mice. Immunity. 2018;49(5):971–e865. https://doi.org/10.1016/j.immuni.2018.09.009.
60. Wang Z, Xie L, Ding G, Song S, Chen L, Li G, et al. Single-cell RNA sequencing of peripheral blood mononuclear cells from acute Kawasaki disease patients. Nat Commun. 2021;12(1):5444. https://doi.org/10.1038/s41467-021-25771-5.
61. Griffiths P, Reeves M. Pathogenesis of human cytomegalovirus in the immunocompromised host. Nat Rev Microbiol. 2021;19(12):759–73. https://doi.org/10.1038/s41579-021-00582-z.
62. Mitchell DA, Xie W, Schmittling R, Learn C, Friedman A, McLendon RE et al. Sensitive detection of human cytomegalovirus in tumors and peripheral blood of patients diagnosed with glioblastoma. Neuro Oncol. 2008;10(1):10–8. https://doi.org/10.1215/15228517-2007-035.
63. Schiemann U, Kellner H. Specific localisation of human cytomegalovirus nucleic acids and proteins in human colorectal cancer. Z Gastroenterol. 2003;41(8):881–2. https://doi.org/10.1055/s-2003-41205.
64. Samanta M, Harkins L, Klemm K, Britt WJ, Cobbs CS. High prevalence of human cytomegalovirus in prostatic intraepithelial neoplasia and prostatic carcinoma. J Urol. 2003;170(3):998–1002. https://doi.org/10.1097/01.ju.0000080263.46164.97.
65. Xing Y, Wang Y, Wang S, Wang X, Fan D, Zhou D, et al. Human cytomegalovirus infection contributes to glioma disease progression via upregulating endocan expression. Transl Res. 2016;177:113–26. https://doi.org/10.1016/j.trsl.2016.06.008.
66. El Baba R, Pasquereau S, Haidar Ahmad S, Monnien F, Abad M, Bibeau F, et al. EZH2-Myc driven glioblastoma elicited by cytomegalovirus infection of human astrocytes. Oncogene. 2023;42(24):2031–45. https://doi.org/10.1038/s41388-023-02709-3.
67. Santarelli R, Arteni AMB, Gilardini Montani MS, Romeo MA, Gaeta A, Gonnella R, et al. KSHV dysregulates bulk macroautophagy, mitophagy and UPR to promote endothelial to mesenchymal transition and CCL2 release, key events in viral-driven sarcomagenesis. Int J Cancer. 2020;147(12):3500–10. https://doi.org/10.1002/ijc.33163.
68. Goncalves PH, Ziegelbauer J, Uldrick TS, Yarchoan R. Kaposi sarcoma herpesvirus-associated cancers and related diseases. Curr Opin HIV AIDS. 2017;12(1):47–56. https://doi.org/10.1097/COH.0000000000000330.
69. Mesri EA, Cesarman E, Boshoff C. Kaposi's sarcoma and its associated herpesvirus. Nat Rev Cancer. 2010;10(10):707–19. https://doi.org/10.1038/nrc2888.
70. Hsu YC, Huang DQ, Nguyen MH. Global burden of hepatitis B virus: current status, missed opportunities and a call for action. Nat Rev Gastroenterol Hepatol. 2023;20(8):524–37. https://doi.org/10.1038/s41575-023-00760-9.

71. Ghafouri-Fard S, Safarzadeh A, Taheri M, Jamali E. Identification of diagnostic biomarkers via weighted correlation network analysis in colorectal cancer using a system biology approach. Sci Rep. 2023;13(1):13637. https://doi.org/10.1038/s41598-023-40953-5.
72. Thomsen H, Chen B, Figlioli G, Elisei R, Romei C, Cipollini M, et al. Runs of homozygosity and inbreeding in thyroid cancer. BMC Cancer. 2016;16:227. https://doi.org/10.1186/s12885-016-2264-7.
73. Yu Y, Krupa A, Keesler RI, Grinwis GCM, de Ruijsscher M, de Vos J, et al. Familial follicular cell thyroid carcinomas in a large number of Dutch German longhaired pointers. Vet Comp Oncol. 2022;20(1):227–34. https://doi.org/10.1111/vco.12769.
74. Jing J, Wu Z, Wang J, Luo G, Lin H, Fan Y, et al. Hedgehog signaling in tissue homeostasis, cancers, and targeted therapies. Signal Transduct Target Ther. 2023;8(1):315. https://doi.org/10.1038/s41392-023-01559-5.
75. Jiang J. Hedgehog signaling mechanism and role in cancer. Semin Cancer Biol. 2022;85:107–22. https://doi.org/10.1016/j.semcancer.2021.04.003.
76. Engelman JA, Cantley LC. The role of the ErbB family members in non-small cell lung cancers sensitive to epidermal growth factor receptor kinase inhibitors. Clin Cancer Res. 2006;12(14 Pt 2):4372s–6s. https://doi.org/10.1158/1078-0432.CCR-06-0795.
77. Tanabe A, Tanikawa K, Tsunetomi M, Takai K, Ikeda H, Konno J, et al. RNA helicase YTHDC2 promotes cancer metastasis via the enhancement of the efficiency by which HIF-1α mRNA is translated. Cancer Lett. 2016;376(1):34–42. https://doi.org/10.1016/j.canlet.2016.02.022.
78. Tanabe A, Nakayama T, Kashiyanagi J, Yamaga H, Hirohashi Y, Torigoe T, et al. YTHDC2 Promotes Malignant Phenotypes of Breast Cancer Cells. J Oncol. 2022;2022:9188920. https://doi.org/10.1155/2022/9188920.
79. He JJ, Li Z, Rong ZX, Gao J, Mu Y, Guan YD, et al. m6A Reader YTHDC2 Promotes Radiotherapy Resistance of Nasopharyngeal Carcinoma via Activating IGF1R/AKT/S6 Signaling Axis. Front Oncol. 2020;10:1166. https://doi.org/10.3389/fonc.2020.01166.
80. Wang W, Sun B, Xia Y, Sun S, He C. RNA N6-Methyladenosine-Related Gene Contribute to Clinical Prognostic Impact on Patients With Liver Cancer. Front Genet. 2020;11:306. https://doi.org/10.3389/fgene.2020.00306.
81. Liu J, Wang D, Zhou J, Wang L, Zhang N, Zhou L, et al. N6-methyladenosine reader YTHDC2 and eraser FTO may determine hepatocellular carcinoma prognoses after transarterial chemoembolization. Arch Toxicol. 2021;95(5):1621–9. https://doi.org/10.1007/s00204-021-03021-3.
82. Wang W, Li J, Lin F, Guo J, Zhao J. Identification of N6-methyladenosine-related lncRNAs for patients with primary glioblastoma. Neurosurg Rev. 2021;44(1):463–70. https://doi.org/10.1007/s10143-020-01238-x.
83. Wu Q, Xie X, Huang Y, Meng S, Li Y, Wang H, et al. N6-methyladenosine RNA methylation regulators contribute to the progression of prostate cancer. J Cancer. 2021;12(3):682–92. https://doi.org/10.7150/jca.46379.
84. Yuan W, Chen S, Li B, Han X, Meng B, Zou Y, et al. The N6-methyladenosine reader protein YTHDC2 promotes gastric cancer progression via enhancing YAP mRNA translation. Transl Oncol. 2022;16:101308. https://doi.org/10.1016/j.tranon.2021.101308.
85. Deng C, Ye C, Liao X, Zhou F, Shi Y, Zhong H, et al. KMT2A maintains stemness of gastric cancer cells through regulating Wnt/β-catenin signaling-activated transcriptional factor KLF11. Open Med. 2023;18(1):20230764. https://doi.org/10.1515/med-2023-0764.
86. Fang Y, Zhang D, Hu T, Zhao H, Zhao X, Lou Z, et al. KMT2A histone methyltransferase contributes to colorectal cancer development by promoting cathepsin Z transcriptional activation. Cancer Med. 2019;8(7):3544–52. https://doi.org/10.1002/cam4.2226.
87. Zhao W, Lin J, Cheng S, Li H, Shu Y, Xu C. Comprehensive analysis of COMMD10 as a novel prognostic biomarker for gastric cancer. PeerJ. 2023;11:e14645. https://doi.org/10.7717/peerj.14645.
88. Goldberg Y, Aleme O, Peled-Perets L, Castellvi-Bel S, Nielsen M, Shalev SA. MCM9 is associated with germline predisposition to early-onset cancer-clinical evidence. NPJ Genom Med. 2021;6(1):78. https://doi.org/10.1038/s41525-021-00242-4.
89. Portolés I, Ribera J, Fernandez-Galán E, Lecue E, Casals G, Melgar-Lesmes P, et al. Identification of Dhx15 as a Major Regulator of Liver Development, Regeneration, and Tumor Growth in Zebrafish and Mice. Int J Mol Sci. 2024;25(7):3716. https://doi.org/10.3390/ijms25073716.
90. Wang YH, Huang JH, Tu JF, Wu MH. MED27 promotes malignant behavior of cells by affecting Sp1 in breast cancer. Eur Rev Med Pharmacol Sci. 2020;24(12):6802–8. https://doi.org/10.26355/eurrev_202006_21669.
91. Iansante V, Choy PM, Fung SW, Liu Y, Chai JG, Dyson J, et al. PARP14 promotes the Warburg effect in hepatocellular carcinoma by inhibiting JNK1-dependent PKM2 phosphorylation and activation. Nat Commun. 2015;6:7882. https://doi.org/10.1038/ncomms8882.
92. Berg HE, Greipp PT, Baughn LB, Falcon CP, Jackson CC, Peterson JF. Detection of a Cryptic KMT2A/AFDN Gene Fusion [ins(6;11)(q27;q23q23)] in a Pediatric Patient with Newly Diagnosed Acute Myeloid Leukemia. Lab Med. 2022;53(4):e95–9. https://doi.org/10.1093/labmed/lmab109.
93. Chen Y, Chen X, Pan L, Huang Y, Cai Y, Li J, et al. RNA helicase DHX15 decreases cell apoptosis by NF-κB signaling pathway in Burkitt lymphoma. Cancer Cell Int. 2022;22(1):92. https://doi.org/10.1186/s12935-021-02426-5.
94. Han X, Liu H, Tang X, Zhao Y. Knockdown of mediator complex subunit 27 suppresses gastric cancer cell metastasis and angiogenesis via Wnt/β-catenin pathway. Tissue Cell. 2022;79:101973. https://doi.org/10.1016/j.tice.2022.101973.
95. Dubovik T, Lukačišin M, Starosvetsky E, LeRoy B, Normand R, Admon Y, et al. Interactions between immune cell types facilitate the evolution of immune traits. Nature. 2024;632(8024):350–6. https://doi.org/10.1038/s41586-024-07661-0.
96. Kumar MP, Du J, Lagoudas G, Jiao Y, Sawyer A, Drummond DC, et al. Analysis of Single-Cell RNA-Seq Identifies Cell-Cell Communication Associated with Tumor Characteristics. Cell Rep. 2018;25(6):1458–e684. https://doi.org/10.1016/j.celrep.2018.10.047.
97. Huang M, Xu L, Liu J, Huang P, Tan Y, Chen S. Cell-Cell Communication Alterations via Intercellular Signaling Pathways in Substantia Nigra of Parkinson's Disease. Front Aging Neurosci. 2022;14:828457. https://doi.org/10.3389/fnagi.2022.828457.
98. Han B, Fang T, Zhang Y, Zhang Y, Gao J, Xue Y. Association of the TGFβ gene family with microenvironmental features of gastric cancer and prediction of response to immunotherapy. Front Oncol. 2022;12:920599. https://doi.org/10.3389/fonc.2022.920599.
99. Lemma EY, Letian A, Altorki NK, McGraw TE. Regulation of PD-L1 Trafficking from Synthesis to Degradation. Cancer Immunol Res. 2023;11(7):866–74. https://doi.org/10.1158/2326-6066.CIR-22-0953.
100. Krizbai IA, Gasparics Á, Nagyőszi P, Fazakas C, Molnár J, Wilhelm I, et al. Endothelial-mesenchymal transition of brain endothelial cells: possible role during metastatic extravasation. PLoS ONE. 2015;10(3):e0119655. https://doi.org/10.1371/journal.pone.0119655.
101. Nie L, Lyros O, Medda R, Jovanovic N, Schmidt JL, Otterson MF, et al. Endothelial-mesenchymal transition in normal human esophageal endothelial cells cocultured with esophageal adenocarcinoma cells: role of IL-1β and TGF-β2. Am J Physiol Cell Physiol. 2014;307(9):C859–77. https://doi.org/10.1152/ajpcell.00081.2014.
102. Kim SH, Song Y, Seo HR. GSK-3β regulates the endothelial-to-mesenchymal transition via reciprocal crosstalk between NSCLC cells and HUVECs in multicellular tumor spheroid models. J Exp Clin Cancer Res. 2019;38(1):46. https://doi.org/10.1186/s13046-019-1050-1.
103. Wawro ME, Chojnacka K, Wieczorek-Szukała K, Sobierajska K, Niewiarowska J. Invasive Colon Cancer Cells Induce Transdifferentiation of Endothelium to Cancer-Associated Fibroblasts through Microtubules Enriched in Tubulin-β3. Int J Mol Sci. 2018;20(1):53. https://doi.org/10.3390/ijms20010053.
104. Timmins MA, Ringshausen I. Transforming Growth Factor-Beta Orchestrates Tumour and Bystander Cells in B-Cell Non-Hodgkin Lymphoma. Cancers. 2022;14(7):1772. https://doi.org/10.3390/cancers14071772.
105. Tian W, Zhu Y, Wang Y, Teng F, Zhang H, Liu G, et al. Visfatin, a potential biomarker and prognostic factor for endometrial cancer. Gynecol Oncol. 2013;129(3):505–12. https://doi.org/10.1016/j.ygyno.2013.02.022.
106. Shi J, Li Q, Li J, Zhou J, Zhang X, Wang S, et al. Single-Cell RNA Sequencing Reveals the Spatial Heterogeneity and Functional Alteration of Endothelial Cells in Chronic Hepatitis B Infection. Int J Mol Sci. 2024;25(13):7016. https://doi.org/10.3390/ijms25137016.
107. Luo W, Quan Q, Xu Z, Lei J, Peng R. Bioinformatics analysis of MMP14 + myeloid cells affecting endothelial-mesenchymal transformation and immune microenvironment in glioma. Heliyon. 2024;10(5):e26859. https://doi.org/10.1016/j.heliyon.2024.e26859.
108. Kampa M, Notas G, Stathopoulos EN, Tsapis A, Castanas E. The TNFSF Members APRIL and BAFF and Their Receptors TACI, BCMA, and BAFFR in Oncology, With a Special Focus in Breast Cancer. Front Oncol. 2020;10:827. https://doi.org/10.3389/fonc.2020.00827.
109. Ng LG, Mackay CR, Mackay F. The BAFF/APRIL system: life beyond B lymphocytes. Mol Immunol. 2005;42(7):763–72. https://doi.org/10.1016/j.molimm.2004.06.041.
110. Jasek M, Bojarska-Junak A, Sobczyński M, Wagner M, Chocholska S, Roliński J, et al. Association of Common Variants of TNFSF13 and TNFRSF13B Genes with CLL Risk and Clinical Picture, as Well as Expression of Their Products-APRIL

and TACI Molecules. Cancers. 2020;12(10):2873. https://doi.org/10.3390/cancers12102873.
111. Notas G, Alexaki VI, Kampa M, Pelekanou V, Charalampopoulos I, Sabour-Alaoui S, et al. APRIL binding to BCMA activates a JNK2-FOXO3-GADD45 pathway and induces a G2/M cell growth arrest in liver cells. J Immunol. 2012;189(10):4748–58. https://doi.org/10.4049/jimmunol.1102891.
112. Yoo SA, Leng L, Kim BJ, Du X, Tilstam PV, Kim KH, et al. MIF allele-dependent regulation of the MIF coreceptor CD44 and role in rheumatoid arthritis. Proc Natl Acad Sci U S A. 2016;113(49):E7917–26. https://doi.org/10.1073/pnas.1612717113.
113. Liu PS, Chen YT, Li X, Hsueh PC, Tzeng SF, Chen H, et al. CD40 signal rewires fatty acid and glutamine metabolism for stimulating macrophage anti-tumorigenic functions. Nat Immunol. 2023;24(3):452–62. https://doi.org/10.1038/s41590-023-01430-3.
114. Liu FT, Stowell SR. The role of galectins in immunity and infection. Nat Rev Immunol. 2023;23(8):479–94. https://doi.org/10.1038/s41577-022-00829-7.

## Publisher's note